PCCP

Accepted Manuscript

ROYAL SOCIETY OF CHEMISTRY

www.rsc.org/pccp

Physical Chemistry Chemical Physics RSCPublishing

ARTICLE

Surface-Charge Accumulation Effects on Open-Circuit Voltage in Organic Solar Cells Based on Photoinduced Impedance Analysis

Huidong Zang, Yu-Che Hsiao, and Bin Hu*

The accumulation of dissociated charge carriers plays an important role in reducing the loss occurring in organic solar cells. We find from light-assisted capacitance measurements that the charge accumulation inevitably occurred at the electrode and photovoltaic layer interface for bulk-heterojunction ITO/PEDOT/P3HT:PCBM/Ca/Al solar cells. Our results indicate, for the first time through impedance measurement, that the charge accumulation exists at the anode side of the device, and more importantly, we successfully identify the type of charge accumulated. Further study shows that the charge accumulation can significantly affect open circuit voltage and short circuit current. As a result, our experimental results from light assisted capacitance measurements provide a new understanding on the loss in open-circuit voltage and short-circuit photocurrent based on charge accumulation. Clearly, controlling charge accumulation presents a new mechanism to improve photovoltaic performance in organic solar cells.

Introduction

Organic photovoltaic devices have attracted intensive attention due to the unique features such as mechanical flexibilities, facile materials processing, and low costs. Recent research developments have demonstrated high photovoltaic efficiencies with the values around 10% in organic solar cells.[1-10] These advancements can be attributed to both materials synthesis and device engineering. In particular, recent experimental studies have shown that inserting a dielectric layer can lead to a large enhancement on photovoltaic efficiencies in organic solar cells.[11-14] Our early experimental studies have found that photogenerated charge carriers can inevitably accumulate at photovoltaic/electrode interfaces upon charge transport to respective electrodes.[15-17] Obviously, the charge accumulation generates a photovoltaic loss when an organic solar cell is under operation. The impedance spectroscopy is widely used to investigate the interfacial properties of organic solar cells.[18-22] Here, we found from photoinduced impedance studies that accumulated charge carriers can modify the effective potential barrier at photovoltaic layer/electrode interface in organic solar cells under device-operating condition. Furthermore, we observed that the accumulated charge carriers can affect the open-circuit voltage (V_{oc}) when the effective interfacial potential is changed by charge accumulation. It is known that the V_{oc} is the photovoltage reflecting the energy conversion from photoexcitation to electricity; and both experimental and theoretical studies have been performed, finding that the V_{oc} is essentially determined by the charge-transfer states[23, 24] and/or the polarization effects[25, 26] between donor and acceptor molecular interfaces. We find through photoinduced impedance studies that the V_{oc} change that the modification on potential barrier at photovoltaic layer/electrode interface caused by charge accumulation can directly change the energy conversion from photoexcitation to electricity in organic solar cells.

Results and discussion

Figure 1 shows the capacitance-voltage (CV) characteristics for the ITO/PEDOT:PSS/P3HT:PCBM/Ca/Al device at different light illumination intensities from 0.1 sun (10 mW/cm^2) to 1 sun (100 mW/cm^2) before and after thermal annealing. It has been well studied that thermal annealing can improve the morphological structures in the P3HT:PCBM film and also the interfacial contact of photovoltaic film with electrodes, and consequently enhances the photovoltaic performance by increasing exciton dissociation and charge transport.[27-33] Here, our purpose is to use CV properties as an experimental tool to characterize the surface accumulation of photogenerated charge carriers and to investigate the effects of surface charge accumulation on Voc by comparing annealed and un-annealed P3HT:PCBM devices. Based on thermal annealing-induced modification on bulk morphological structures and interfacial contacts in the P3HT:PCBM device, the CV characteristics can then reveal the surface accumulation of photogenerated charge carriers and the effects of surface charge accumulation on the effective interfacial potential barrier in the development of V_{oc}. We can see from **Figure 1** that the P3HT:PCBM device shows a larger shift of CV peak (V_{peak}), when the photoexcitation increases from 0.1 sun to 1 sun, after thermal annealing as compared to the situation before thermal annealing. The following analysis indicates that a larger V_{peak} shift corresponds to a more accumulation of photogenerated charge carriers at the interfaces in the P3HT:PCBM solar cell. Here, we discuss three details from the CV characteristics. First, the device capacitance under photoexcitation is increased when the applied bias is swept from negative to positive value towards V_{peak} at both conditions before and after thermal annealing. Sweeping the applied bias towards V_{peak} value provides an external electric field against the built-in electric field, leading to a reduction on effective field strength between ITO and Al electrodes to drift photogenerated carriers to respective electrodes. The capacitance increase essentially reflects that the photogenerated charge carriers become more accumulated on the surfaces of photovoltaic film when the applied bias is swept towards V_{peak}. Second, the charge accumulation reaches a maximum value at the V_{peak} voltage. Further increasing forward bias beyond the V_{peak} value can clearly reduce the device capacitance. The decrease in device capacitance indicates that an applied bias larger than the V_{peak} value can cause a charge injection, in the direction against the transport of photogenerated carriers, to initiate charge recombination inside the device. Therefore, the V_{peak} value can be used to evaluate the effective potential barrier for realizing the charge injection at electrode interfaces under device-operating condition. Third, the V_{peak} value is decreased as photoexcitation intensity increases from 0.1 sun to 1 sun, leading to a V_{peak} shift. Furthermore, the device before and after annealing exhibits smaller and larger V_{peak} shifts (0.10 V and 0.19 V), respectively. By combining the above-mentioned three experimental results, we can suggest that the accumulation of photogenerated charge carriers decreases the effective barriers at electrode interfaces in the P3HT:PCBM device under operation condition.

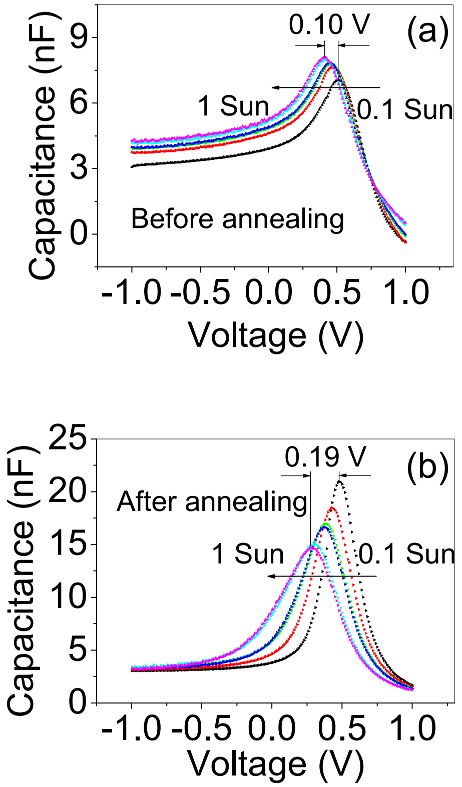

Figure 1. The capacitance-voltage characteristics for P3HT:PCBM solar cell at different photoexcitation intensities from 0.1 sun to 1 sun. The P3HT:PCBM weight ratio is 1:0.8. (a): before annealing. (b): after thermal annealing.

The reduction on interfacial potential barriers due to the accumulation of photogenerated carriers can be discussed as follows. In the metal-semiconductor contact, the dark injection barrier can be described by the following equation[34]

$$n_i = N_t \exp\left(-\frac{\phi_i}{k_B T}\right) \tag{1}$$

where the n_i is the surface charge density, N_t is the volume density of molecular sites, ϕ_i is the potential barrier at the interface between active medium and the electrode. Apparently, a higher surface charge density corresponds to a lower potential barrier ϕ_i. We should note that the surface charge density is decided by both injected carriers (namely dark carriers) from electrodes and photogenerated carriers accumulated at photovoltaic layer/electrode interfaces when applied bias initiates injection current at V_{peak} condition. As a result, increasing the intensity of the incident light can increase the accumulation of photogenerated charge carriers at photovoltaic layer/electrode interfaces and then lead to a reduction of the interfacial potential barrier. Clearly, the accumulation of photogenerated carriers can decrease the effective potential barriers at photovoltaic layer/electrode interfaces and consequently shift the V_{peak}.

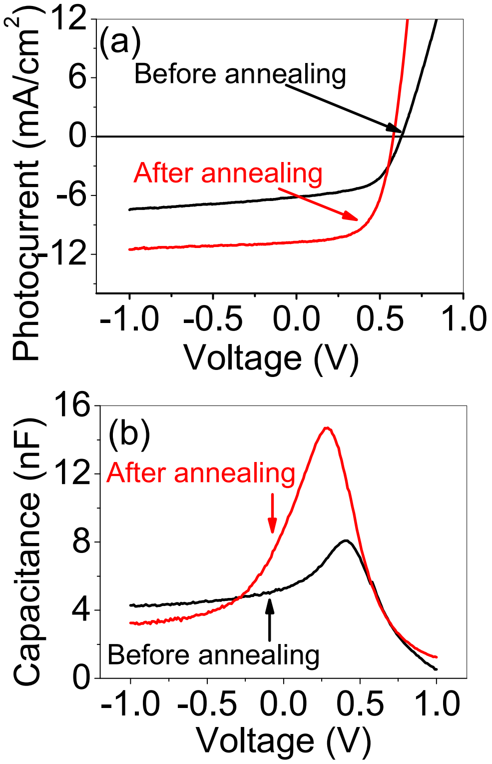

Figure 2. The I-V (a) and CV (b) characteristics at 1 sun condition for P3HT:PCBM solar cell before and after thermal annealing.

It has been commonly observed that thermal annealing can lead to a reduction on V_{oc} while the power conversion efficiencies are increased in organic solar cells.[35-38] **Figure 2** (a) shows that the V_{oc} decreases from 0.63 V to 0.58 V in the P3HT:PCBM cell after thermal annealing. The J_{sc} after thermal annealing increases from 6.2 mA/cm^2 to 10.8 mA/cm^2, and the power conversion efficiency changes from 2.2% to 3.7%. It has been reported that thermal annealing can change surface energy levels and consequently modifies the V_{oc}.[39-41] Here, our analysis indicates that the increased surface charges from the accumulation of photogenerated carriers are a new factor that can reduce the V_{oc} upon thermal annealing by decreasing the effective potential barriers at photovoltaic layer/electrode interfaces. **Figure 2** (b) shows the CV characteristics for the P3HT:PCBM device before and after thermal annealing under 1 sun photoexcitation. It can be seen that the V_{peak} shifts to a low voltage from 0.42 V to 0.29 V after thermal annealing. Especially, the P3HT:PCBM device before and after annealing exhibits smaller and larger V_{peak} changing rates: 44 mV/[mW/cm^2] and 87 mV/[mW/cm^2] in **Figure 3**. This V_{peak} shift confirms that the effective potential barriers at photovoltaic layer/electrode interfaces are decreased by thermal annealing. The capacitance increase at zero bias caused by thermal annealing further supports our argument that the surface charge density is increased by the accumulation of photogenerated carriers through morphological development upon thermal annealing.

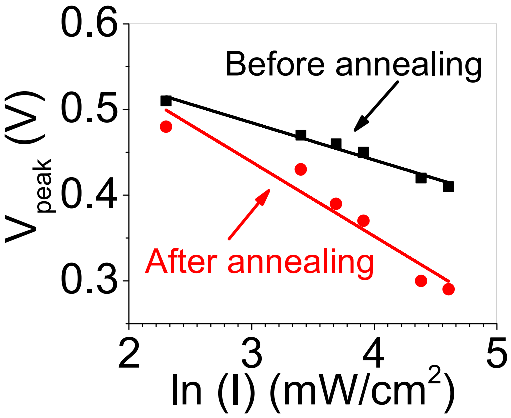

Figure 3. Vpeak characteristics at different photoexcitation intensities for P3HT:PCBM solar cell before and after thermal annealing. The solid lines are the linear fitting for Vpeak before (black) and after (red) thermal annealing.

Now we discuss the type of photogenerated carriers: either photogenerated electrons or holes, are accumulated to form surface charges which modify the effective potential barrier at the photovoltaic layer/electrode interfaces. The CV studies have provided powerful techniques to study dynamic processes in organic solar cells under device-operating condition.[34, 42-46] However, the type of photogenerated charge carriers accumulated at photovoltaic layer/electrode interfaces has not been explored through CV analysis. We know that at the charge injection occurs at V_{peak} condition. The V_{peak} essentially reflects the effective potential barrier at a given photoexcitation intensity. Increasing the photoexcitation intensity can decrease the effective potential barrier and consequently reduces the V_{peak} due to the accumulation of photogenerated charge carriers. **Figure 3** shows that the V_{peak} shift (from 0.48 V to 0.29 V) after thermal annealing is much larger than that (from 0.51 V to 0.41 V) before thermal annealing when the photoexcitation intensity changes from 0.1 sun to 1 sun. This means that the charge accumulation becomes more significant after thermal annealing as the photoexcitation intensity approaches to 1 sun. We should note that the literature reports have shown that thermal annealing can increase the hole mobility by three orders in the P3HT:PCBM device, while the electron mobility did not show significant change.[47, 48] We can therefore propose that the photogenerated holes are the carriers that form surface charges through accumulation with the consequence of modifying the effective potential barrier on the surface of hole-collecting electrode (ITO/PEDOT:PSS). This proposed hypothesis can be confirmed by the following experimental results based on p-type P3HT:PCBM composite device. The p-type P3HT:PCBM device was fabricated with donor-rich P3HT and acceptor-deficit PCBM design with PCBM weight ratio relative to P3HT at 0 wt%, 5 wt% and 10 wt%, respectively. These p-type devices can exhibit two particular properties: (i) low concentration of photogenerated carriers due to the limited PCBM doping and (ii) sufficient hole transport channel but in-sufficient electron transport channel. In these p-type devices we can only consider the transport of photogenerated holes. We can theoretically expect that with the increase of PCBM doping level, the appreciable V_{peak} shift can

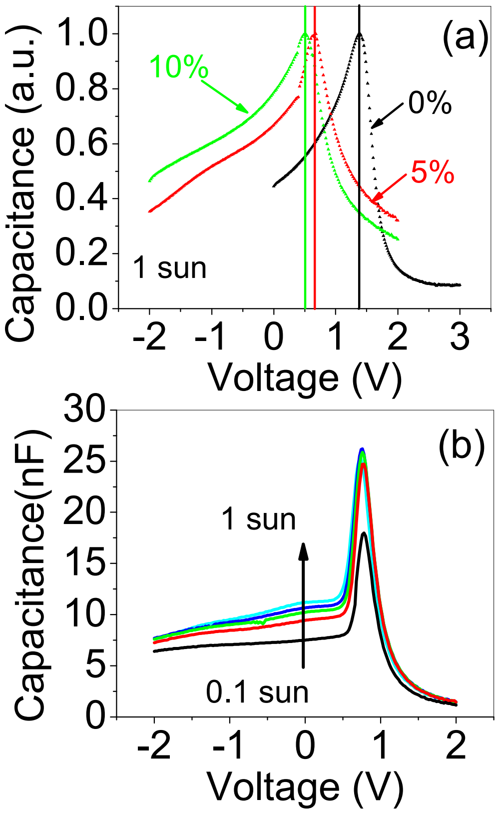

Figure 4. (a) Normalized C-V characteristics for p-type P3HT:PCBM devices with 0 wt%, 5 wt% and 10 wt% PCBM doping concentration at 1 sun condition. (b) C-V characteristics for n-type P3HT:PCBM devices with 10 wt% P3HT doping in PCBM under different light illumination intensities.

be developed due to the fact of more efficient photoinduced charge (hole) accumulation when increasing the PCBM concentration.

Figure 4 (a) shows the C-V results for these p-type devices measure at 1 sun condition. We can see a significant V_{peak} shift with the different PCBM doping levels. As discussed above, the 5 wt% and 10 wt% PCBM doping in P3HT cannot form efficient PCBM networks, thus the electron transportation is limited. However, the holes have a decent transport channel due to the formation of P3HT networks in the bulk heterojunction structures. Thus, the holes have larger probabilities to accumulate at the interface between the anode and photovoltaic layer when they are transported towards the anode for charge collection. In other words, the V_{peak} shift can be attributed to the hole accumulation at anode interface. It is noted from **Figure 4 (a)** that the V_{peak} shift for the devices with 5 wt% and 10 wt% PCBM doping levels are 0.71V and 0.88V, respectively, while the pristine P3HT device shows the V_{peak} of 1.38V. This result is also consistent with the V_{peak} shift in optimized device (80 wt% PCBM doping in P3HT), in which the larger V_{peak} shifts of 0.97V, and 1.09V were observed for un-annealed and annealed situations (see **Figure 3**). Moreover, an n-type device is fabricated and conducted under CV measurement with 10 wt% P3HT doping in PCBM. The CV peaks for the n-type device is shown in **Figure 4 (b)**. The V_{peak} is found to be 0.78V and it did not shift with increasing light intensity, which is because increasing light intensity cannot significantly change both the charge generation, due to both the deficit of photon absorber (P3HT), and the charge (hole) accumulation at the interface due to the lack of hole transport channel. Therefore, we can experimentally confirm our hypothesis: the surface charge accumulation comes from the photogenerated holes in the P3HT:PCBM device.

Here, we further analyze the relation between the V_{oc} and V_{peak} to understand effects of surface charges on photovoltaic parameters in organic solar cells. **Figure 5** shows the difference (V_{oc} - V_{peak}) as a function of photoexcitation intensity ranging from 0.1 sun to 1 sun before and after thermal annealing. It is observed that the difference (V_{oc} - V_{peak}) is linearly dependent on the light intensity in logarithmic scale. By combining C-V and I-V characteristics at different photoexcitation intensities, the relationship between V_{oc} and V_{peak} can be established by

$$V_{oc} - V_{peak} = \frac{nKT}{e} \cdot \ln\frac{J_{sc}}{J_{00}} \qquad (2)$$

where n is the morphology related factor, K is the Boltzmann constant, T is the absolute temperature, and J_{00} is the characteristic current. For P3HT:PCBM system, fitting the experimental data in **Figure 5** can give the specific relationship between V_{oc} and V_{peak} for the situations before annealing (Eq. (3)) and after annealing (Eq. (4)).

$$V_{oc} - V_{peak} = \frac{2.9KT}{e} \cdot \ln\frac{J_{sc}}{0.38} \qquad (3)$$

$$V_{oc} - V_{peak} = \frac{4.8KT}{e} \cdot \ln\frac{J_{sc}}{1.17} \qquad (4)$$

Therefore, we can see that the surface charges reflected by Vpeak can affect the Voc and Jsc, and consequently the power conversion efficiencies in organic solar cells.

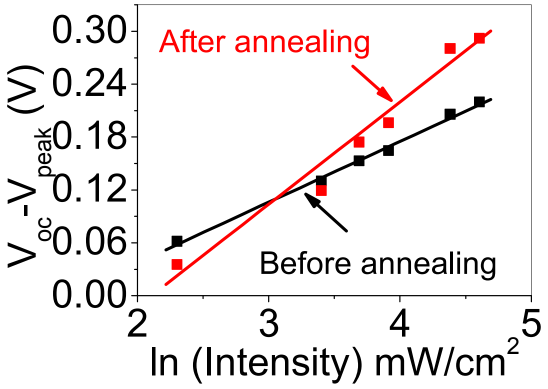

Figure 5. V_{oc}-V_{peak} versus logarithmic photoexcitation intensity for P3HT:PCBM cell (1:0.8 weight ratio) before and after thermal annealing. The solid lines are the simulation from Eq. (3) and Eq. (4).

Conclusions

In summary, the photoinduced impedance measurements were used to study the surface charges and effective potential barriers to understand the effects of charge accumulation on key photovoltaic parameters based on the P3HT:PCBM system. We observed from the CV characteristics that the accumulation of photogenerated carriers can inevitably occur at photovoltaic/electrode interfaces to form surface charges. Furthermore, we found that the surface charges can decrease the effective potential barriers and consequently reduces the V_{oc} when the injection current balances the photocurrent J_{sc}. By adjusting the transport of photogenerated holes in the CV characteristics, we confirmed that the surface charges comes from the accumulation of photogenerated holes at the interface between photovoltaic film and hole-collecting electrode. Moreover, we established the relationship between V_{peak} and V_{oc} to understand the effects of charge accumulation on key photovoltaic parameters in organic solar cells.

Experimental

The regioregular poly(3-methylthiophene) (P3HT) and fullerene derivative 1-(3-methyloxycarbonyl)-propyl-1-phenyl (6,6) C61 (PCBM) were used as recieved from Rieke Metal, Inc. and Nano-C, Inc., respectively. The average molecular weight of P3HT is 50,000. The chlorobenzene was used as the solvent to disovle the P3HT:PCBM composite for spin coating photovoltaic films with the thickness around 100 nm in nitrigen atomsphere. The hole-transporting layer (polyethylenedioxythiophene/polystyrenesulphonate (PEDOT/PSS)) was spin cast with the thickness of 40 nm on previuosly cleaned ITO subsrates. The Ca and Al were thermally deposited under the vacuum of 7×10^{-7} Torr. The current-voltage characteristics were measured by using Keithley 2400 source meter with sunlight simulator (Thermal Oriel 96000 300 W from Newport). Thermal annealing was carried out in a nitrogen atmosphere by heating the P3HT:PCBM devices at 155 ℃ for 5 minutes. The CV measurements were performed by using dielectric spectrometer (Agilent; E4980A) at different photoexcitation intensities

Acknowledgements

The authors would like to acknowledge the financial supports from NSF Under grant numbers ECCS-0644945 and ECCS-1102011. This research was partially conducted at the Center for Nanophase Materials Sciences based on user project (CNMS2012-106 and CNMS2012-107), which is sponsored at Oak Ridge National Laboratory by the Division of Scientific User Facilities, U.S. Department of Energy. This research was also supported by International Cooperation and Exchange Program (Gant No.21161160445) and photovoltaic project (Grant No. 61077020) funded by the National Natural Science Foundation of China. The authors also acknowledge the support from National Significant Program (Quantum Control: 2013CB922104).

Notes and reference

Department of Materials Science and Engineering, University of Tennessee, Knoxville, 37996, USA. Email: bhu@utk.edu

Present address for Dr. Huidong Zang: Center for Functional Nanomaterials, Brookhaven National Laboratory, Upton, NY, 11973, USA

References

1. Z. He, C. Zhong, S. Su, M. Xu, H. Wu and Y. Cao, *Nature Photonics*, 2012, **6**, 593-597.
2. J. You, L. Dou, K. Yoshimura, T. Kato, K. Ohya, T. Moriarty, K. Emery, C. C. Chen, J. Gao, G. Li and Y. Yang, *Nature communications*, 2013, **4**, 1446.
3. L. Dou, W.-H. Chang, J. Gao, C.-C. Chen, J. You and Y. Yang, *Advanced Materials*, 2013, **25**, 825-831.
4. G. Zhao, Y. He and Y. Li, *Adv Mater*, 2010, **22**, 4355-4358.
5. E. Wang, L. Hou, Z. Wang, S. Hellström, F. Zhang, O. Inganäs and M. R. Andersson, *Advanced Materials*, 2010, **22**, 5240-5244.
6. Y. Liang, Z. Xu, J. Xia, S.-T. Tsai, Y. Wu, G. Li, C. Ray and L. Yu, *Advanced Materials*, 2010, **22**, E135-E138.
7. R. Qin, W. Li, C. Li, C. Du, C. Veit, H.-F. Schleiermacher, M. Andersson, Z. Bo, Z. Liu, O. Ingana□s, U. Wuerfel and F. Zhang, *Journal of the American Chemical Society*, 2009, **131**, 14612-14613.
8. S. H. Park, A. Roy, S. Beaupre, S. Cho, N. Coates, J. S. Moon, D. Moses, M. Leclerc, K. Lee and A. J. Heeger, *Nat Photon*, 2009, **3**, 297-302.
9. J. Hou, H.-Y. Chen, S. Zhang, R. I. Chen, Y. Yang, Y. Wu and G. Li, *Journal of the American Chemical Society*, 2009, **131**, 15586-15587.
10. M.-S. Su, C.-Y. Kuo, M.-C. Yuan, U. S. Jeng, C.-J. Su and K.-H. Wei, *Advanced Materials*, 2011, **23**, 3315-3319.
11. N. Li, T. Stubhan, D. Baran, J. Min, H. Q. Wang, T. Ameri and C. J. Brabec, *Adv Energy Mater*, 2013, **3**, 301-307.
12. S. Kwon, J. K. Park, G. Kim, J. Kong, G. C. Bazan and K. Lee, *Adv Energy Mater*, 2012, **2**, 1420-1424.
13. J. Yang, R. Zhu, Z. Hong, Y. He, A. Kumar, Y. Li and Y. Yang, *Adv Mater*, 2011, **23**, 3465-3470.
14. X. Liu, H. Kim and L. J. Guo, *Organic Electronics*, 2013, **14**, 591-598.
15. H. D. Zang, Z. H. Xu and B. Hu, *Journal of Physical Chemistry B*, 2010, **114**, 5704-5709.
16. H. Zang, Y. Liang, L. Yu and B. Hu, *Adv Energy Mater*, 2011, **1**, 923-929.
17. Z. H. Xu, H. D. Zang and B. Hu, *Jom-Us*, 2008, **60**, 49-53.
18. C. Melzer, E. J. Koop, V. D. Mihailetchi and P. W. M. Blom, *Adv Funct Mater*, 2004, **14**, 865-870.
19. W. L. Leong, S. R. Cowan and A. J. Heeger, *Adv Energy Mater*, 2011, **1**, 517-522.
20. I. Mora-Seró, J. Bisquert, F. Fabregat-Santiago, G. Garcia-Belmonte, G. Zoppi, K. Durose, Y. Proskuryakov, I. Oja, A. Belaidi, T. Dittrich, R. Tena-Zaera, A. Katty, C. Lévy-Clément, V. Barrioz and S. J. C. Irvine, *Nano Letters*, 2006, **6**, 640-650.
21. S. K. Hau, H.-L. Yip, O. Acton, N. S. Baek, H. Ma and A. K. Y. Jen, *Journal of Materials Chemistry*, 2008, **18**, 5113-5119.
22. C. Lungenschmied, E. Ehrenfreund and N. S. Sariciftci, *Organic Electronics*, 2009, **10**, 115-118.
23. K. Vandewal, K. Tvingstedt, A. Gadisa, O. Inganäs and J. V. Manca, *Physical Review B*, 2010, **81**, 125204.
24. K. Vandewal, K. Tvingstedt, A. Gadisa, O. Inganas and J. V. Manca, *Nature Materials*, 2009, **8**, 904-909.
25. E. B. Isaacs, S. Sharifzadeh, B. Ma and J. B. Neaton, *The Journal of Physical Chemistry Letters*, 2011, **2**, 2531-2537.
26. B. M. Wong and T. H. Hsieh, *Journal of Chemical Theory and Computation*, 2010, **6**, 3704-3712.
27. W. L. Ma, C. Y. Yang, X. Gong, K. Lee and A. J. Heeger, *Adv Funct Mater*, 2005, **15**, 1617-1622.
28. H. Chen, S. Hu, H. Zang, B. Hu and M. Dadmun, *Adv Funct Mater*, 2013, **23**, 1701-1710.
29. C.-Y. Kuo, M.-S. Su, G.-Y. Chen, C.-S. Ku, H.-Y. Lee and K.-H. Wei, *Energy & Environmental Science*, 2011, **4**, 2316-2322.
30. W.-R. Wu, U. S. Jeng, C.-J. Su, K.-H. Wei, M.-S. Su, M.-Y. Chiu, C.-Y. Chen, W.-B. Su, C.-H. Su and A.-C. Su, *ACS Nano*, 2011, **5**, 6233-6243.
31. E. Verploegen, R. Mondal, C. J. Bettinger, S. Sok, M. F. Toney and Z. Bao, *Adv Funct Mater*, 2010, **20**, 3519-3529.
32. M. A. Ruderer, S. Guo, R. Meier, H.-Y. Chiang, V. Körstgens, J. Wiedersich, J. Perlich, S. V. Roth and P. Müller-Buschbaum, *Adv Funct Mater*, 2011, **21**, 3382-3391.
33. R. Hegde, N. Henry, B. Whittle, H. Zang, B. Hu, J. Chen, K. Xiao and M. Dadmun, *Solar Energy Materials and Solar Cells*, 2012, **107**, 112-124.
34. S. L. van Mensfoort and R. Coehoorn, *Physical review letters*, 2008, **100**, 086802.
35. T.-F. Guo, T.-C. Wen, G. L'Vovich Pakhomov, X.-G. Chin, S.-H. Liou, P.-H. Yeh and C.-H. Yang, *Thin Solid Films*, 2008, **516**, 3138-3142.
36. J. Liu, Y. Shi and Y. Yang, *Adv Funct Mater*, 2001, **11**, 420-424.
37. P. Vanlaeke, A. Swinnen, I. Haeldermans, G. Vanhoyland, T. Aernouts, D. Cheyns, C. Deibel, J. D'Haen, P. Heremans, J. Poortmans and J. V. Manca, *Solar Energy Materials and Solar Cells*, 2006, **90**, 2150-2158.

38. E. A. Katz, D. Faiman, S. M. Tuladhar, J. M. Kroon, M. M. Wienk, T. Fromherz, F. Padinger, C. J. Brabec and N. S. Sariciftci, *Journal of Applied Physics*, 2001, **90**, 5343-5350.
39. T. Nagamori and K. Marumoto, *Advanced Materials*, 2013, **25**, 2362-2367.
40. W. C. Tsoi, S. J. Spencer, L. Yang, A. M. Ballantyne, P. G. Nicholson, A. Turnbull, A. G. Shard, C. E. Murphy, D. D. C. Bradley, J. Nelson and J.-S. Kim, *Macromolecules*, 2011, **44**, 2944-2952.
41. T. M. Clarke, A. M. Ballantyne, J. Nelson, D. D. C. Bradley and J. R. Durrant, *Adv Funct Mater*, 2008, **18**, 4029-4035.
42. A. Guerrero, L. F. Marchesi, P. P. Boix, S. Ruiz-Raga, T. Ripolles-Sanchis, G. Garcia-Belmonte and J. Bisquert, *ACS Nano*, 2012, **6**, 3453-3460.
43. S. Lee, J.-H. Lee, K. H. Kim, S.-J. Yoo, T. G. Kim, J. W. Kim and J.-J. Kim, *Organic Electronics*, 2012, **13**, 2346-2351.
44. P. P. Boix, J. Ajuria, R. Pacios and G. Garcia-Belmonte, *Journal of Applied Physics*, 2011, **109**, 074514-074515.
45. M. Bag and K. S. Narayan, *Physical Review B*, 2010, **82**, 075308.
46. C. Melzer, E. Koop, V. Mihailetchi and P. Blom, *Adv Funct Mater*, 2004, **14**, 865-870.
47. V. D. Mihailetchi, H. X. Xie, B. de Boer, L. J. A. Koster and P. W. M. Blom, *Adv Funct Mater*, 2006, **16**, 699-708.
48. D. Veldman, S. C. J. Meskers and R. A. J. Janssen, *Adv Funct Mater*, 2009, **19**, 1939-1948.